JOURNAL OF PROPULSION AND POWER
Vol. 26, No. 4, July–August 2010

Technical Notes

Operating Radio Frequency Antennas Immersed in Vacuum: Implications for Ground-Testing Plasma Thrusters

Michael D. West,* Christine Charles,† and Rod W. Boswell‡
Australian National University,
Canberra, Australian Capital Territory 0200, Australia

DOI: 10.2514/1.49384

Nomenclature

A_s	=	area of antenna sheath, m^2
A_w	=	area of vacuum chamber wall, m^2
C_{block}	=	blocking capacitor, nF
C_1	=	tunable capacitor, pF
C_2	=	tunable capacitor, pF
Q	=	quality factor, arbitrary units
r	=	radial position, cm
V_{bias}	=	antenna self-bias, kV
V_p	=	plasma potential, V
V_{rf}	=	radio frequency voltage, V
z	=	axial position, cm

I. Introduction

OPERATING RF antennas in a vacuum presents several challenges that are relevant to the ground testing of plasma propulsion systems such as the Helicon Double Layer Thruster (HDLT) prototype. Antennas immersed in vacuum can come into contact with the plasma and, if one end of the antenna is grounded, direct currents flow from the plasma to ground. To the authors' knowledge, these issues have not been investigated previously in the context of plasma propulsion. However, in asymmetric plasma discharges, which are used in materials processing, the RF biased substrate or electrodes are frequently immersed in the vacuum (and plasma) and biased negatively via a dc blocking capacitor. This enables the energies of the ions impinging the substrate to be controlled independently of the current to the substrate, which is important for various processing techniques [1]. Immersed RF antennas have also been employed in plasma immersion ion implantation (PI^3) devices [2].

In magnetically confined fusion experiments, the RF antennas are usually shielded with a Faraday cage to prevent the antenna from coming into contact with the plasma. This shielding reduces the power coupling of the plasma to the antenna and hence the efficiency of the system. The RF antenna in the H1 Heliac experiment [3], however, is in direct contact with the plasma and is used to increase the temperature of the plasma. The antenna, which is driven at 7 MHz, is shaped like a loop in the plane of the last closed flux surface, and one end of the antenna is grounded. This allows a direct current to flow from the plasma via the antenna to ground. Currents of approximately 90 A and plasma potentials of 100 V have been measured during typical operation of the H1 Heliac.

The HDLT is a new plasma propulsion concept based on the discovery by various researchers of energetic ion beams formed by a current-free electric double layer in low-pressure helicon plasmas [4,5]. The HDLT is electrodeless, does not require a neutralizer, can operate with a wide variety of propellants [6,7] and produces a very-low-divergence ion beam (less than 10° for argon and 6° for xenon) [8] that can be steered magnetically [9,10]. A prototype of the HDLT has been developed and an initial testing campaign was conducted in the CORONA space simulation chamber [11]. This has been followed by a more extensive testing program with the HDLT prototype immersed in a smaller vacuum chamber [12–14].

In this work, several deleterious phenomena are described that have been observed during this testing program. To alleviate these problems, modifications to the RF (13.56 MHz) matching box and antenna assembly have been implemented. These phenomena, their consequences, and the solutions implemented here are also relevant to ground testing other plasma thrusters such as the new VASIMR VX-200 prototype [15] and other concepts using RF or helicon antennas [16–24].

II. Experimental Setup

The HDLT prototype and the vacuum chamber in which it is installed have been described previously [12] and are shown in Fig. 1. In brief, the vacuum chamber is 1 m in diameter and 1.4 m long and has a base pressure less than 1.2×10^{-4} Pa (9×10^{-7} torr) with an effective pumping speed measured for argon of approximately 330 Ls^{-1} and 210 Ls^{-1} for xenon. The HDLT prototype was originally designed for the European Space Research and Technology Centre testing campaign [11] and consists of a Pyrex source tube (5 mm wall thickness), with a closed end of Pyrex, that has an outer diameter of 15 cm and has a length, and hence insulating plasma cavity, of 29 cm. The end of the HDLT structure is at $z = 0$ cm and the end of the HDLT source tube, which is the exit of the thruster, is at $z = 3$ cm. A divergent magnetic field is produced by the solenoids of the HDLT prototype that has an on-axis maximum magnitude of 138 G at $z = -5$ cm that decreases to less than 5 G at the wall of the downstream end of the vacuum chamber ($z = 83$ cm). The applied magnetic field remains constant for all experiments in this study.

The HDLT source tube is surrounded by a double-saddle field helicon antenna, based on that invented by Boswell [25,26], which is constructed from copper with a 25 μm silver plating. The antenna is supplied with RF power at 13.56 MHz via a custom-built L impedance-matching network located on the outside of the vacuum chamber. The matching network shares a ground with the vacuum chamber. The quality of the impedance match is measured upstream of the matching network. The antenna is considered matched when the standing wave ratio is less than 1.2. The matching box and antenna assembly are described further in Sec. VI. The argon or xenon propellant is injected via nylon tubing that enters the source at the closed Pyrex end. For all experiments in this study, the flow rate remained constant at 0.297 mg s^{-1} (10 sccm), which resulted in an operating pressure of 59.9 mPa (0.45 mtorr).

A standard uncompensated planar Langmuir probe with a 3-mm-diam disc tip is installed axially via the end port of the vacuum chamber. It is attached directly to a Tektronix TDS1012B Digital Storage oscilloscope that enables time resolved measurements of the floating potential to be made. Since the Langmuir probe is only used in this study to determine the floating potential and not the electron

Received 16 February 2010; revision received 13 April 2010; accepted for publication 14 April 2010.

*Ph.D. Candidate, Space Plasma, Power and Propulsion Group, Research School of Physics and Engineering; michael@rwts.com.au. Member AIAA.
†Associate Professor, Space Plasma, Power and Propulsion Group, Research School of Physics and Engineering; christine.charles@anu.edu.au.
‡Professor, Space Plasma, Power and Propulsion Group, Research School of Physics and Engineering.

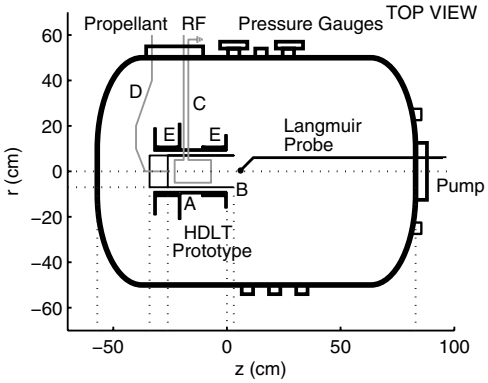

Fig. 1 HDLT prototype installed inside the vacuum chamber with the Langmuir probe shown. The HDLT prototype consists of the HDLT structure (A), the Pyrex source tube (B), shielded copper rods attached to a double-saddle field antenna (C), a nylon propellant line (D), and two solenoids (E).

temperature or the electron energy distribution function, an RF-compensated Langmuir probe is unnecessary. The probe tip is positioned on the centerline of the vacuum chamber at $r = 0$ cm and downstream of the thruster exit at $z = 6$ cm (Fig. 1). A Tektronix P6015A 1000×3.0 pF 100 MΩ passive high-voltage probe, connected to a HP54600A oscilloscope, is affixed to the matching box circuit and used to measure the self-bias on the antenna, V_{bias}.

III. Microarcing

As the RF power applied to the HDLT prototype is increased from 100 to 500 W, it was found that many small pinpoint discharges appeared on the inside of the walls of the vacuum chamber. This often observed but rarely discussed phenomenon is known as microarcing [27,28] and is not specific to this experiment and is more predominant in low-temperature plasmas. Microarcing has been attributed to the breakdown of the sheath at the vacuum chamber wall as a result of an increase in the plasma and floating potentials [29,30]. As illustrated in Fig. 2, the immersed antenna is powered by an RF voltage of amplitude V_{rf}, has an area of A_s, is in direct contact with the plasma, and is dc-grounded. The wall of the vacuum chamber is also grounded and has an area of A_w. Here, $A_w \gg A_s$ and so the impedance of the sheath on the immersed antenna dominates that of the walls of the chamber because of their vastly different areas and hence capacitances.

Figure 2 shows the voltage distribution in the system at various times throughout the RF cycle. At the immersed antenna, when the applied RF voltage, $V_{\text{rf}}(t) = V_{\text{rf}} \cos(\omega t)$, is at a maximum (position 1 in Fig. 2), the instantaneous plasma potential $V_p(t)$ is at its maximum and is lower than the RF amplitude V_{rf}. This results in an electron current flow from the plasma towards the immersed antenna. Conversely, $V_p(t)$ is much larger than V_{rf} when $V_{\text{rf}}(t)$ is most negative and an ion current flows from the plasma to the immersed antenna. With each RF cycle, the magnitude of the electron current

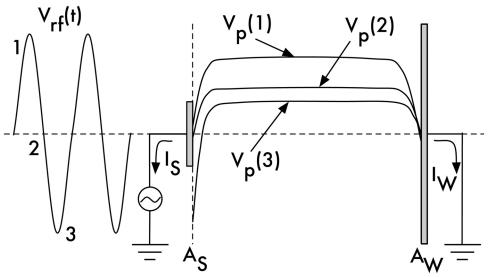

Fig. 2 Schematic of the voltage distributions around the small immersed antenna (left) and the large vacuum chamber wall (right) at various times during the RF cycle.

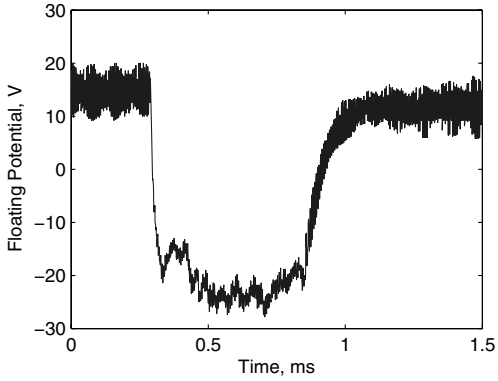

Fig. 3 Floating potential vs time during a microarc event.

drawn over the positive half-cycle is much larger than that of the ion current drawn over the negative half-cycle and the net negative charge escapes from the plasma via the grounded antenna. Since charge equilibrium can not be maintained, the plasma potential will rise progressively as electrons are lost without a corresponding loss of ions. Eventually, the plasma potential will rise to such a point that the plasma sheath at the chamber wall can not be maintained and the sheath rapidly collapses resulting in an arc breakdown at the chamber wall [31].

The microarcs result in a large release of energy over a small area at the chamber wall over the space of a millisecond or less. These discharges can damage sensitive electrical components and interfere with diagnostic measurements as they affect the bulk plasma parameters. At the location of the microarc, metallic vapor and other impurities are also released, which can result in undesirable coatings being deposited on the vacuum chamber, on the propulsion system being tested, and on any plasma diagnostics. Examination of the walls of the vacuum chamber revealed many examples of pitting as a result of these microarcs. Pitting has also been observed on the surfaces of electrostatic probes and the target plate of a momentum-flux measuring instrument [32] placed in the plasma.

To investigate the microarcing phenomena, time resolved measurements were made of the floating potential using the Langmuir probe with the probe tip positioned on the centerline of the vacuum chamber at $r = 0$ cm and downstream of the thruster exit at $z = 6$ cm. An example of the results obtained is shown in Fig. 3. It is clear that as a microarc event begins the floating potential drops rapidly by approximately -35 V and continues to decrease as the microarcing event progresses. Once the arcing event stops, the charging process rebuilds the floating potential and the floating potential increases exponentially with a typical time constant of ~ 50 μs, which is much longer than the RF period (~ 72 ns) and is related to the ion diffusion time, as described elsewhere [33]. This continues until the floating potential increases enough to trigger another microarc event. The microarcing was observed to be quasi-periodic with large discharges followed by smaller ones. The arcing frequency was found to increase with increased RF power and also with a decrease in the operating pressure. These observations are consistent with the observations of other researchers [27,28].

IV. Formation of Unwanted Plasmas

When attempting to operate at greater than 500 W or at high flow rates and operating pressures [greater than 0.4 Pa (3 mtorr) with argon and greater than only 26.6 mPa (0.2 mtorr) with xenon], the plasma discharge would escape from inside the HDLT source tube and preferentially form around the antenna in the cavity between the HDLT structure (labeled A in Fig. 1) and the HDLT source tube (labeled B in Fig. 1). This obviously prevents the HDLT prototype from being operated as desired in the present configuration. This phenomenon also produces lots of small discharges and sparking on the grounded HDLT structure and damages this structure as well as the antenna. Burn marks and discoloration were also observed on the HDLT structure and the antenna.

In some other instances, even when the plasma was contained inside the HDLT source tube and matched correctly, a separate small localized plasma was observed around the antenna. This parasitic plasma, as it is called here, affects the tuning of the plasma within the thruster cavity, introduces random noise into the match and can cause the matching of the RF system to change erratically. The parasitic plasma also results in some sputtering of the silver coating that is on the antenna (or of the copper antenna itself if not silver-coated). The amount of RF power transferred or coupled to the plasma formed in the HDLT source is also reduced as a result of the parasitic plasma and this makes it difficult to assess the actual power input into the HDLT prototype and, consequently, its power efficiency.

V. Possible Solutions

To minimize the challenges associated with microarcing and parasitic plasma formation and enable the HDLT prototype to be operated at higher RF powers and flow rates, the current path on the antenna to ground must be removed or limited. One option described by other researchers [34] is direct current magnetic insulation of the immersed RF antenna to reduce the potential difference between the plasma and the antenna via the application of a dc current to the antenna. The dc current produces a magnetic field next to the antenna. It is proposed that this magnetic field traps electrons that would normally escape the plasma and flow to the antenna. An alternative approach is to use a floating antenna configuration that has been investigated by several groups and has been shown to limit microarcing and other detrimental phenomena [27–31,35]. The installation of a blocking capacitor would allow the immersed antenna to float and to develop an appropriate negative self-bias [33], which would enhance the negative voltage excursion and reduce the positive voltage excursion with respect to the plasma potential. This should bring the electron and ion currents into equilibrium and limit sheath breakdown and microarcing. The installation of a blocking capacitor to the matching box is reasonably straight forward and so this approach was adopted here. For reference, during the initial tests of the HDLT prototype in the CORONA facility [11], the RF antenna was grounded and no blocking capacitor was installed.

VI. Matching Box Modifications and Consequences

A 9 nF blocking capacitor, C_{block}, was added to the matching network to act as a dc block, isolate the antenna from ground and allow the antenna to develop a negative self-bias with current flowing only during the charge-up stage of the capacitor (some tens of microseconds). As a result, the plasma potential is prevented from rising, the sheath does not break down, and hence the instances of microarcing decrease. It should be noted that with this additional capacitor, the matching circuit is still resonant and the tuning of the impedance-matching network is not affected significantly. The measured Q factor with and without the blocking capacitor is unchanged ($Q \sim 8$) for a 130 W argon plasma and the plasma potential inside the main cavity and the ion beam properties are unchanged. Large voltages still exist on the antenna, but the voltage is shifted down by V_{bias}.

Figure 4 shows a schematic of the modified matching network circuit and the antenna assembly immersed in vacuum. For reference, the tunable capacitors C_1 and C_2 are rated for 50 and 2000 pF, respectively, and therefore $C_{\text{block}} \gg C_1$ and C_2. The measured inductance of the antenna assembly, including the two copper rods and the vacuum feedthrough, is 9.5 μH. With the blocking capacitor installed, it was possible to safely increase the RF power beyond 500 W without the entire plasma escaping from the HDLT source and forming around the antenna. Yet, some small parasitic plasmas were still observed around the antenna. The instances of microarcing also decreased significantly as a result of installing the blocking capacitor.

However, the installation of a blocking capacitor does have some consequences. Since the Q factor is unchanged, large negative self-biases form on the antenna, which enhance the negative voltage excursions on the antenna during each RF cycle. This causes ions in the small parasitic plasma outside the plasma cavity to be accelerated by the sheath and flow towards the antenna. These ions bombard the antenna and sputter the silver surfaces [35]. Since the sputtering rate is a function of the energy of the bombarding ions, the greater the magnitude of the antenna self-bias, the greater the rate at which the silver is removed from the antenna.

Using the high-voltage probe, as shown in Fig. 4, V_{bias} was measured as a function of RF power when operating with xenon, and the results are shown in Fig. 5. The magnitude of the self-bias on the immersed antenna increases with the RF power, which is consistent with observations in other helicon systems [29,35]. The dashed line in Fig. 5 indicates the RF power at which the plasma transitions to the high-density xenon mode that is discussed in detail elsewhere [13]. In this high-density mode, the magnitude of V_{bias} decreases as the matching of the plasma changes dramatically, the plasma resistance increases and more RF power is deposited into the plasma. Visual inspection of the HDLT source tube after continued operation in the high-density mode revealed that less sputtered silver was deposited on the HDLT source tube compared to when operating for extended periods at lower RF powers. This observation is consistent with the measured decrease in the antenna self-bias when operating at higher RF powers in the high-density mode (Fig. 5).

If not managed correctly, the sputtered silver can accumulate on the HDLT source tube, the HDLT structure and the antenna electrical connectors. These layers of silver can create unwanted paths to ground. The sputtered silver can also cause damage to the antenna and other components as well as change the plasma parameters dramatically. The sputtered silver can also coat the ceramic spacers that are used to affix the antenna to the grounded HDLT structure, once again creating unwanted paths to ground. When this occurs, the power from the antenna shorts to the HDLT structure and the plasma can not be ignited and tuned correctly. To minimize this problem, ceramic discs with a diameter larger than the ceramic spacers were added to act like an umbrella and protect the ceramic spacers from being coated with the sputtered silver. This proved to be an effective strategy for minimizing the unwanted

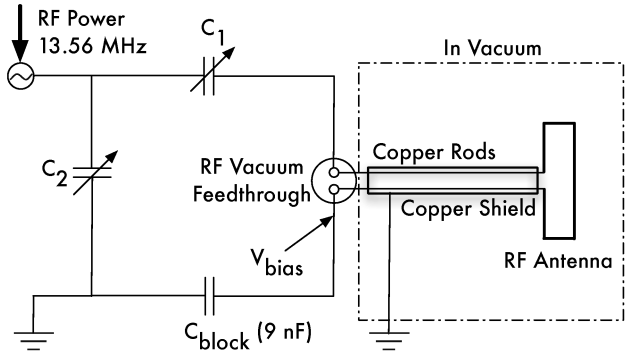

Fig. 4 Schematic of the matching box circuit showing the tunable capacitors C_1 and C_2, the dc blocking capacitor C_{block} and where V_{bias} is measured.

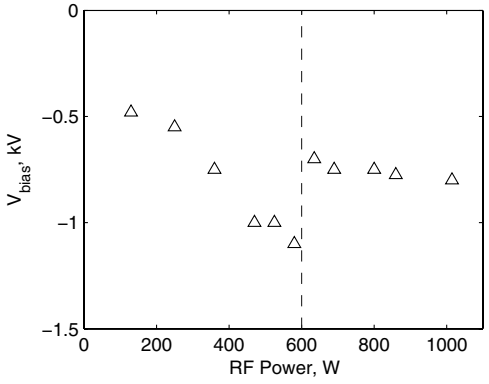

Fig. 5 Antenna bias voltage measured between the RF vacuum feedthrough and the blocking capacitor on the matching box versus RF power when operating at 0.45 mtorr with xenon.

electrical pathways to the grounded HDLT structure and allow the HDLT prototype to operate and be characterized over a larger range of external parameters (higher RF powers, higher flow rates, etc.). However, it should be noted that sputtering of the antenna is undesirable and could cause erosion and eventual failure of the antenna. Possible solutions, which should be investigated in the future, include coating the antenna with a sacrificial ceramic insulator and sealing off the cavity between the HDLT structure and the source tube where the antenna resides. This second approach would prevent residual gas from entering the cavity and stop the formation of the parasitic plasma.

VII. Conclusions

In this work, several of the challenges associated with operating the RF antenna of the HDLT prototype immersed in a vacuum have been discussed. Small discharges observed inside the vacuum chamber have been identified as microarcs caused by the collapse of the sheath at the wall of the vacuum chamber. Several detrimental effects caused by the microarcing were observed, including the deposition of coatings on components inside the vacuum chamber and the pitting of the walls of the chamber. The formation of unwanted plasmas around the antenna has also been observed, and as a result, the range of RF powers and gas flow rates that the HDLT prototype could operate over is restricted.

To alleviate these problems, the matching box circuit was modified via the installation of a blocking capacitor, in order to float the RF antenna. As a result, large negative self-biases form on the antenna that induce sputtering of the silver coating of the antenna. The sputtered silver produced unwanted electrical paths that damaged the antenna and other components and therefore additional modifications were made to the antenna to mitigate this problem. The modifications described in this work have enabled consistent and uninterrupted operation of the HDLT prototype at higher RF powers and higher flow rates with both argon and xenon gas than that previously attainable. These experiences highlight some of the issues that will need to be considered for future designs of the HDLT and that are also applicable to the design of other electric propulsion systems that use RF antennas.

References

[1] Lieberman, M. A., and Litchtenberg, A. J., *Principles of Plasma Discharges and Materials Processing*, 2nd ed., Wiley-Interscience, New York, 2005.

[2] Collins, G. A., and Tendys, J., "Measurement Of Potentials and Sheath Formation in Plasma Immersion Ion Implantation," *Journal of Vacuum Science and Technology B (Microelectronics and Nanometer Structures)*, Vol. 12, No. 2, 1994, pp. 875–879. doi:10.1116/1.587363

[3] Hamberger, S. M., Blackwell, B. D., Sharp, L. E., and Shenton, D. B., "H-1 Design and Construction," *Fusion Technology*, Vol. 17, No. 1, 1990, pp. 123–130.

[4] Charles, C., and Boswell, R. W., "Current-Free Double Layer Formation in a High-Density Helicon Discharge," *Applied Physics Letters*, Vol. 82, No. 9, 2003, pp. 1356–1358. doi:10.1063/1.1557319

[5] Cohen, S. A., Siefert, N. S., Stange, S., Bolvin, R. F., Scime, E. E., and Levinton, F. M., "Ion Acceleration in Plasmas Emerging from a Helicon-Heated Magnetic-Mirror Device," *Physics of Plasmas*, Vol. 10, No. 6, 2003, pp. 2593–2598. doi:10.1063/1.1568342

[6] Charles, C., Boswell, R. W., Laine, R., and MacLellan, P., "An Experimental Investigation of Alternative Propellants for the Helicon Double Layer Thruster," *Journal of Physics D: Applied Physics*, Vol. 41, 2008, Paper 175213. doi:10.1088/0022-3727/41/17/175213

[7] Charles, C., "Plasmas for Spacecraft Propulsion," *Journal of Physics D: Applied Physics*, Vol. 42, 2009, Paper 163001. doi:10.1088/0022-3727/42/16/163001

[8] Cox, W., Charles, C., Boswell, R. W., and Hawkins, R., "Spatial Retarding Field Energy Analyzer Measurements Downstream of a Helicon Double Layer Plasma," *Applied Physics Letters*, Vol. 93, 2008, Paper 071505. doi:10.1063/1.2965866

[9] Charles, C., Boswell, R. W., Cox, W., Laine, R., and MacLellan, P., "Magnetic Steering of a Helicon Double Layer Thruster," *Applied Physics Letters*, Vol. 93, 2008, Paper 201501. doi:10.1063/1.3033201

[10] Cox, W., Charles, C., Boswell, R. W., Laine, R., and Perren, M., "Asymmetric Magnetic Field Induced Ion Beam Deflection of the Helicon Double Layer Thruster," *Journal of Propulsion and Power* (to be published).

[11] Charles, C., Boswell, R., Alexander, P., Costa, C., Sutherland, O., Pfitzner, L., et al., "Operating the Helicon Double Layer Thruster in a Space Simulation Chamber," *IEEE Transactions on Plasma Science*, Vol. 36, No. 4, Part 1, 2008, pp. 1196–1197. doi:10.1109/TPS.2008.924425

[12] West, M. D., Charles, C., and Boswell, R. W., "Testing a Helicon Double Layer Thruster Immersed in a Space-Simulation Chamber," *Journal of Propulsion and Power*, Vol. 24, No. 1, 2008, pp. 134–141. doi:10.2514/1.31414

[13] West, M. D., Charles, C., and Boswell, R. W., "High Density Mode in Xenon Produced by a Helicon Double Layer Thruster," *Journal of Physics D: Applied Physics*, Vol. 42, 2009, Paper 245201. doi:10.1088/0022-3727/42/24/245201

[14] West, M. D., "Space Simulation Testing of the Helicon Double Layer Thruster Prototype," Ph.D. Thesis, Australian National Univ., Canberra, ACT, Australia, 2009.

[15] Cassady, L. D., Chancery, W. J., Longmier, B. W., Olsen, C., McCaskill, G., Carter, M., et al. "VASIMR Technological Advances and First Stage Performance Results," 45th AIAA/ASME/SAE/ASEE Joint Propulsion Conference, AIAA Paper 2009-5362, 2009.

[16] Choueiri, E. Y., and Polzin, K. A., "Faraday Acceleration with Radio-Frequency Assisted Discharge," *Journal of Propulsion and Power*, Vol. 22, No. 3, 2006, pp. 611–619. doi:10.2514/1.16399

[17] Toki, K., Shinohara, S., Tanikawa, T., and Shamrai, K. P., "Small Helicon Plasma Source for Electric Propulsion," *Thin Solid Films*, Vols. 506–507, 2006, pp. 597–600. doi:10.1016/j.tsf.2005.08.039

[18] Ziemba, T., Euripides, P., Slough, J., Winglee, R., Giersch, L., Carscadden, J., Schnackenberg, T., and Isley, S., "Plasma Characteristics of a High Power Helicon Discharge," *Plasma Sources Science and Technology* , Vol. 15, No. 3, 2006, pp. 517–525. doi:10.1088/0963-0252/15/3/030

[19] Corr, C. S., Zanger, J., Boswell, R. W., and Charles, C., "Ion Beam Formation in a Low-Pressure Geometrically Expanding Argon Plasma," *Applied Physics Letters*, Vol. 91, 2007, Paper 241501. doi:10.1063/1.2823575

[20] Corr, C. S., Boswell, R. W., Charles, C., and Zanger, J., "Spatial Evolution of an Ion Beam Created by a Geometrically Expanding Low-Pressure Argon Plasma," *Applied Physics Letters*, Vol. 92, 2008, Paper 221508. doi:10.1063/1.2938720

[21] Aanesland, A., Meige, A., and Chabert, P., "Electric Propulsion Using Ion-Ion Plasmas," *Journal of Physics: Conference Series*, Vol. 162, 2009, Paper 012009. doi:10.1088/1742-6596/162/1/012009

[22] Palmer, D. D., and Walker, M. L. R., "Operation of an Annular Helicon Plasma Source," *Journal of Propulsion and Power*, Vol. 25, No. 5, 2009, pp. 1013–1019. doi:10.2514/1.41403

[23] Batishchev, O. V., "Minihelicon Plasma Thruster," *IEEE Transactions on Plasma Science*, Vol. 37, No. 8, 2009, pp. 1563–1571. doi:10.1109/TPS.2009.2023990

[24] Virko, V. F., Virko, Y. V., Slobodyan, V. M., and Shamrai, K. P., "The Effect of Magnetic Configuration on Ion Acceleration from a Compact Helicon Source with Permanent Magnets," *Plasma Sources Science and Technology* , Vol. 19, 2010, Paper 015004. doi:10.1088/0963-0252/19/1/015004

[25] Boswell, R. W., "Plasma Production Using a Standing Helicon Wave," *Physics Letters A*, Vol. 33, No. 7, 1970, pp. 457–458. doi:10.1016/0375-9601(70)90606-7

[26] Boswell, R. W., "Very Efficient Plasma Generation by Whistler Waves Near the Lower Hybrid Frequency," *Plasma Physics and Controlled Fusion*, Vol. 26, No. 10, 1984, pp. 1147–1162. doi:10.1088/0741-3335/26/10/001

[27] Yin, Y., Bilek, M. M., McKenzie, D. R., Boswell, R. W., and Charles, C., "Micro-Arcing in Radio Frequency Plasmas," *Journal of Physics D: Applied Physics*, Vol. 37, 2004, pp. 2871–2875. doi:10.1088/0022-3727/37/20/014

[28] Yin, Y., McKenzie, D. R., and Bilek, M. M., "Analytic Analysis on Asymmetrical Micro Arcing in High Plasma Potential RF Plasma

Systems," *Plasma Sources Science and Technology* , Vol. 15, 2006, pp. 99–104.
doi:10.1088/0963-0252/15/1/015

[29] Aanesland, A., Charles, C., Boswell, R. W., and Fredriksen, À., "Helicon Plasma with Additional Immersed Antenna," *Journal of Physics D: Applied Physics*, Vol. 37, 2004, pp. 1334–1341.
doi:10.1088/0022-3727/37/9/006

[30] Aanesland, A., Charles, C., and Boswell, R. W., "Grounded Radio-Frequency Electrodes in Contact with High Density Plasmas," *Physics of Plasmas*, Vol. 12, 2005, Paper 103505.
doi:10.1063/1.2089227

[31] Yin, Y., Bilek, M. M., McKenzie, D. R., Boswell, R. W., and Charles, C., "Microarcing Instability in RF PECVD Plasma System," *Surface and Coatings Technology*, Vol. 198, 2005, pp. 379–383.
doi:10.1016/j.surfcoat.2004.10.089

[32] West, M. D., Charles, C., and Boswell, R. W., "A High Sensitivity Momentum Flux Measuring Instrument for Plasma Thruster Exhausts and Diffusive Plasmas," *Review of Scientific Instruments*, Vol. 80, 2009, Paper 053509.
doi:10.1063/1.3142477

[33] Smith, H. B., Charles, C., Boswell, R. W., and Kuwahara, H., "Bias Formation in a Pulsed Radio Frequency Argon Discharge," *Journal of Applied Physics*, Vol. 82, No. 2, 1997, pp. 561–565.
doi:10.1063/1.365615

[34] Jaworski, M. A., Jurczyk, B. E., Antonsen, E. L., and Ruzic, D. N., "Direct Current Magnetic Insulation of an Immersed RF Antenna," *Plasma Sources Science and Technology* , Vol. 15, 2006, pp. 474–478.
doi:10.1088/0963-0252/15/3/024

[35] Aanesland, A., Charles, C., Boswell, R. W., and Fredriksen, À, "Sputtering Effects in a Helicon Plasma with an Additional Immersed Antenna," *Plasma Sources Science and Technology* , Vol. 12, 2003, pp. 85–88.
doi:10.1088/0963-0252/12/1/311

L. King
Associate Editor